Model validation of tungsten erosion and redeposition properties using biased tungsten samples on DiMES

L. Cappelli, J. Guterl, N. Fedorczak, D.L. Rudakov, G. Sinclair, T. Abrams, S. Di Genova, U. Losada, I. Bykov, Ž. Popović, et al.

Model validation of tungsten erosion and redeposition properties using biased tungsten samples on DiMES

L. Cappelli [a,c,*], J. Guterl [b], N. Fedorczak [c], D.L. Rudakov [d], G. Sinclair [b], T. Abrams [b], S. Di Genova [a], U. Losada [e], I. Bykov [b], Ž. Popović [h], D. Truong [f], J. Watkins [f], R.S. Wilcox [g], W.R. Wampler [f], E. Serre [a]

[a] M2P2 Aix-Marseille Univ, CNRS, Centrale Marseille, 13013, Marseille, France
[b] General Atomics, PO Box 8560, 8, San Diego, CA 92186-5608, USA
[c] CEA, IRFM, F-13108, Saint-Paul-lez-Durance, France
[d] University of California San Diego, 9500 Gilman Drive, 8, La Jolla, CA 92093-0417, USA
[e] Auburn University, 182 S College Street, Auburn, AL 36849, USA
[f] Sandia National Laboratory, PO Box 5800, Albuquerque, NM 87185, USA
[g] Oak Ridge National Laboratory, Oak Ridge, TN 37831-0117, USA
[h] Oak Ridge Associated Universities, Oak Ridge, TN 37830, USA

ARTICLE INFO

Keywords:
Bias
Tungsten
Erosion
Redeposition
ERO2.0

ABSTRACT

An experiment was performed in the DIII-D lower divertor to validate numerical SOL tungsten (W) impurity erosion and redeposition simulations against experimental data. The net and gross erosion of W were calculated as a function of the voltage (or bias) applied to the exposed material. Five samples were inserted into the DIII-D lower divertor using the Divertor Material Evaluation System (DiMES) manipulator and exposed to constant L-mode attached plasma conditions. Each sample was partially coated with W. During plasma shots, samples were biased with respect to the machine vessel ground, ranging from −60 V to 25 V. The ERO2.0 code was used to numerically simulate the experiment aiming to compare the numerical results with experimental measures. A good agreement is found between estimated and measured tungsten erosion at least for negative biases.

1. Introduction

Future magnetic confinement fusion reactors might rely on high-Z metallic plasma-facing components (PFCs) such as tungsten (W), due to their low sputtering yield, high melting point, and low tritium retention [1]. Heavy impurities penetration inside the core causes unacceptable radiative losses. Understanding erosion and its modeling is necessary to design and operate high-Z PFCs. To date, numerical solvers use reduced models necessary to simulate erosion and transport of W without employing heavier simulations (e.g. particle in cell). It is important, however, to validate how well these models can describe the plasma wall interaction and whether there is any need to modify them. To this end, an experiment was performed on the DIII-D lower divertor to validate reduced models embedded in ERO2.0 [2]. The main goal of this work was to experimentally assess the accuracy of current models in evaluating W net and gross erosion as a function of the applied voltage (or bias). In fact, for high-Z elements, net erosion is affected by the electric field inside the plasma sheath [3] which can be manipulated by biasing the target surface.

2. Materials and methods

Five identical samples were inserted into the lower divertor of DIII-D via the Divertor Material Evaluation System (DiMES) [4] as shown in Fig. 1(a). Each sample was exposed to two discharges of an L-mode attached deuterium plasma and biased through a one-spear KEPCO power supply connected to the graphite samples with W coatings (the central part in Fig. 1(a)) electrically insulated from the grounded DiMES holder. After every two shots of exposure, the sample was exchanged and a different voltage was applied. Respectively 25 V, −60 V, 0 V, −40 V, and −20 V were applied, for a total of 10 shots. Biasing was quasi-DC, with regular voltage inversion pulses of 5 ms every 100 ms of constant bias at the nominal value to avoid arcing, as done in [5]. Electron temperature (T_e) and density (n_e) were maintained constant throughout the experiment (see Figs. 2(a) and 2(b) for T_e and n_e profiles). Biased samples consist of a carbon disk of about 0.75 cm in height and 1.9 cm top diameter (with a slightly larger bottom diameter to secure it in the holder) over which 6 W spots with thickness

* Corresponding author at: M2P2 Aix-Marseille Univ, CNRS, Centrale Marseille, 13013, Marseille, France.
E-mail address: luca.cappelli@univ-amu.fr (L. Cappelli).

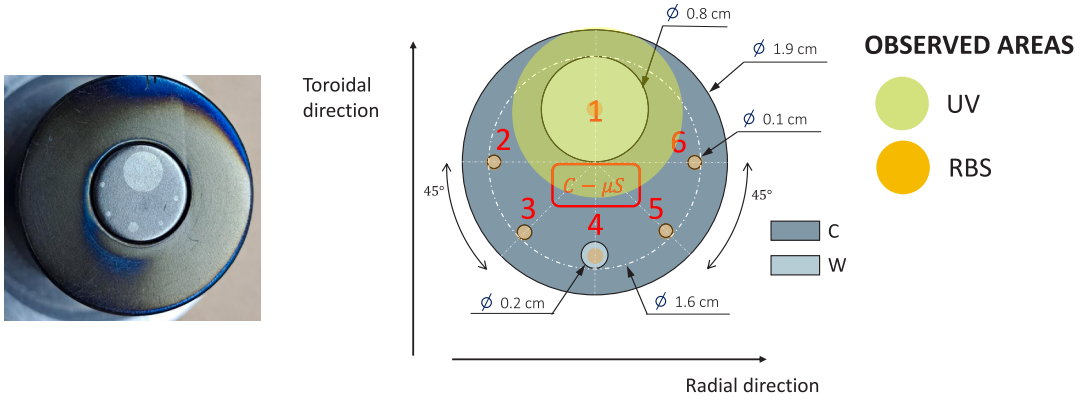

(a) Sample in DiMES (b) Sample design and viewing areas

Fig. 1. DiMES setup top view (a) and viewing spots of the spectroscopy diagnostics employed(b). Also shown are pre and post-exposure RBS measurement locations.

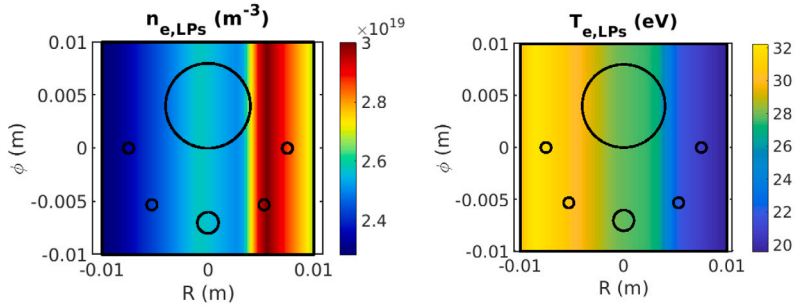

(a) (b)

Fig. 2. Simulated target geometry within ERO2.0. LP measures of n_e at the sheath edge (a) and T_e (b) are here represented.

ranging between 21–27 nm were coated by magnetron sputtering at Sandia National Laboratories. W coatings were enumerated from 1 to 6, number 1 is large compared to the others with a diameter of 8 mm, number 4 is medium-sized being 2 mm in diameter, and the rest (2, 3, 5, and 6) are small with a diameter of 1 mm, see Figs. 1(a) and 1(b). Carbon microspheres (labeled as C-μS in Fig. 1(b)) were manually placed on the carbon substrate to conduct experimental measurements of the incident ions' IAD. The findings from this measure are intended for future research and have not been presented here. Net erosion of the coatings was measured by comparing pre and post-exposure coating thickness via Rutherford Backscattering (RBS) and the gross erosion was estimated by applying the small/large spot technique [6]. Gross erosion was also measured in situ with the Auburn UV spectrometer (255.14 nm neutral W line), and the DiMES-TV (400.88 nm filter) which was excluded due to too low signal. Viewing areas of the UV and RBS are shown in Fig. 1(b).

3. Numerical simulation

3.1. ERO2.0

The Monte Carlo code ERO2.0 [2] was used to numerically estimate the net and gross erosion by tracking the sputtered species as a function of the applied bias. An average grazing impact angle of 80 deg with respect to the normal direction was fixed for the impacting species coming from the plasma, regardless of the bias. This was in line with experimental measures of D impact angle showing that the D Impact Angular Distribution (IAD) has a maximum between 79 and 86 deg [7]. Reflections of incident species over the targets were also considered. The Thompson distribution [8] was adopted for the sputtered particles' energy distribution and a cosinusoidal profile was applied for the angular component. Simulated particles were sampled from a realistic geometry representing the real design (Fig. 2) except made for the carbon substrate that instead of being circular is squared. Particle collisions, thermal forces, drifts, and anomalous diffusion were included. The anomalous diffusion coefficient was set to 1 m^2/s as reported in [9]. Redeposited particles could either reflect or implant into the target causing the mixing of C and W. Each W coating was simulated with a realistic thickness of 30 nm, in line with RBS pre-exposure measures mentioned in Section 2. Reflection coefficients were taken from SDtrimSP databases present in ERO2.0. The surface temperature dynamic and the presence of oxides were not simulated. Finally, the domain was isolated by imposing an absorbing boundary condition, hence, particles reaching the simulation boundary were eliminated.

3.2. Plasma background

A local plasma background of 4 cm^3 over the samples was given as input to the code ERO2.0. Instead of solving it with fluid codes, it was manually designed through assumptions based on experimental data and plasma sheath theory. For instance, considering that the DiMES system in the lower divertor of DIII-D is subjected by a grazing and approximately uniform magnetic field angle $\alpha_B = atan(\frac{\sqrt{B_R^2+B_t^2}}{B_z}) \lesssim 2°$, the radial magnetic component was neglected ($B_t \gg B_R$ at the DiMES location), while B_t and B_z were considered uniform with $\alpha_B = 2°$. The plasma electron density and temperature radial profiles were taken from Langmuir Probes (LP) measurements ($n_{e,LPs}, T_{e,LPs}$) see Fig. 2, the uncertainty for LP measures is around 10%. The electron density variation along the perpendicular axis z was assumed to follow the Boltzmann factor: $n_e(R,\phi,z) = n_{e,LPs}(R)e^{-V(z)/T_e(R\phi,z)}$ Where $V(z)$ is the potential drop along z calculated by ERO2.0 using the fit formula proposed in [10].

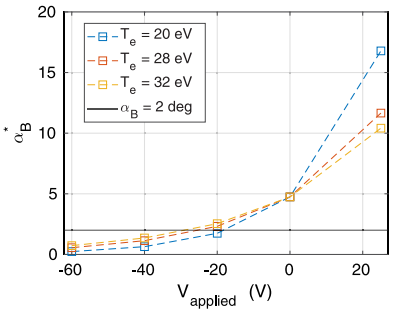

Fig. 3. The critical angle α_B^* for 3 values of T_e if equipartition is considered.

The temperature drop occurring inside the sheath is not considered, thus the electron temperature was considered uniform in the whole domain leading to $T_e(R,\phi,z) = T_{e,LPs}(R)$. Equipartition $T_i = T_{e,LPs}$ and quasi-neutrality were imposed also inside the Debye sheath $n_i = n_e$. Interestingly, at least for null or positive bias the whole plasma background can be quasi-neutral. Indeed, the Debye sheath formation is prevented if the angle α_B is smaller than the critical angle α_B^* [11]. However, in the range of bias explored the Debye sheath reappears already for $V_{applied} = -20\ V$ if equipartition is considered $T_i = T_e$ and $T_e \gtrsim 28$ eV, see Eq. (1) and Fig. 3. Lastly, Carbon was simulated as the only plasma impurity at 2% concentration, and the Carbon population was approximated as 50% C^{+2} and 50% C^{+3} as suggested in previous works [12] for a similar experiment.

$$\alpha_B^* = sin^{-1}\left(\sqrt{2\pi\frac{m_e}{m_i}\left(1+\frac{T_i}{T_e}\right)e^{\frac{V_{applied}}{T_e}}}\right) \quad (1)$$

Where T_e and T_i are in eV, m_i is the main plasma ion mass, m_e is the electron mass, and $V_{applied}$ is the applied voltage.

4. Results

Varying the target surface potential influences the impinging ions' energy and angle of impact, and as a consequence, the sputtering yield. As shown in [13] and [5] the sputtering yield and the gross flux depend on the applied bias, increasing if the bias is negative and decreasing in the opposite case. In the range of bias applied in this work, the same dependence is expected for the net eroded flux. Indeed, the net flux of eroded particles from a finite surface $\Gamma_{net} \approx \Gamma_{gross} \times f_{non-redep}$ where $f_{non-redep}$, is the fraction of non-redeposited W. From [14] $f_{non-redep}$ is directly correlated with the ratio between the neutral W characteristic mean free path $\lambda_{ion} \propto V_{applied}$ and the sheath width λ_{sheath}, hence on the adimensional parameter $\hat{\lambda} = \lambda_{ion}/\lambda_{sheath}$. Anyway, since λ_{sheath} is almost constant in the range of bias applied then also $f_{non-redep}$ and Γ_{net} are expected to be correlated to the bias. For lower biases (higher), $\hat{\lambda}$ increases (decreases) and so will Γ_{net}.

4.1. Net erosion - RBS

RBS was used to compare the thickness of all W coatings before and after the plasma exposure. The difference in thickness can be translated into a net erosion [15], which approximates the gross erosion if the W coating size is small (less than or comparable to the ionization mean free path of the sputtered W atoms) [6]. The net erosion was then converted into a net erosion rate by dividing it by the total exposure time (approximately 8 s). Results for small W coatings (No. 2, 3, 5 and 6) are directly correlated with respect to the applied bias, see Fig. 4(b). Under positive biasing, data points overlap (2 with 3 and 5 with 6), making it challenging to distinguish them visually. Both experimental and numerical results show a radial asymmetry, where the hotter inner side of the sample is more eroded than the outer one, see Fig. 2(b). For both null and positive biasing, the ERO2.0 outcomes consistently underestimate erosion. It is worth noting that RBS accuracy diminishes as the cumulated erosion layers become smaller. Consequently, RBS cannot measure the very small values of net erosion given by ERO2.0. Another point to consider is the possibility that data from coatings 2 to 6 may have been influenced by edge effects. This is because, as illustrated in Fig. 1(a), coatings 2 to 6 were deposited closer to the edge gap between the biased sample and the unbiased DiMES support than originally intended in the design, as depicted in Fig. 1(b). Finally, net erosion rates over the DiMES radial center where n_e and T_e are roughly constant (coatings 1 and 4), do not show a clear trend with respect to the applied bias even if the numerical outcomes are within the experimental uncertainties, see Fig. 4(a). This might be attributed to insufficient statistical data, and additional experiments should be conducted to address this issue more comprehensively.

4.2. Gross erosion - UV

The gross flux from W coating No. 1 was measured with a UV spectrometer looking at the 255.14 nm line. Fluxes were converted into erosion rates assuming W density to be 6.3×10^{22} cm^{-3}. Since two shots were performed for each bias, two different measures are reported when taken, Fig. 5. UV gross erosion measurements are roughly one order of magnitude lower with respect to ERO2.0 results. Moreover, UV gross erosion rates are lower than the net erosion measured with RBS indicating that the associated S/XB, which was calculated with

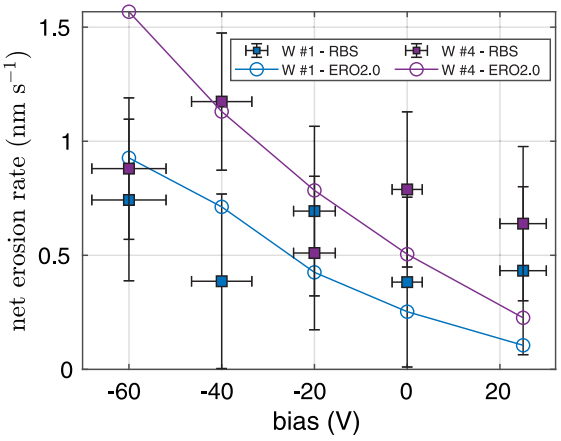

(a) RBS W coatings 1 and 4

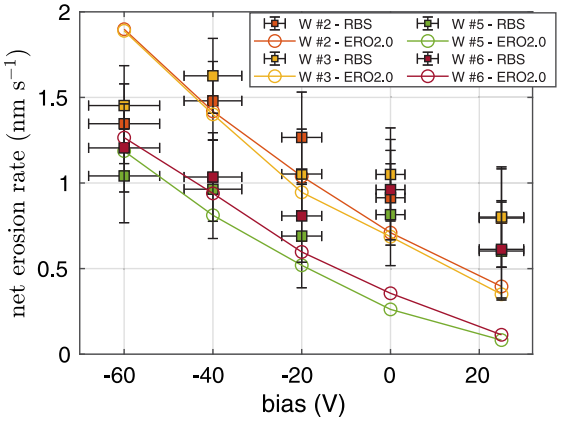

(b) RBS W coatings 2,3,5 and 6

Fig. 4. Resume of RBS experimental measures and simulation results.

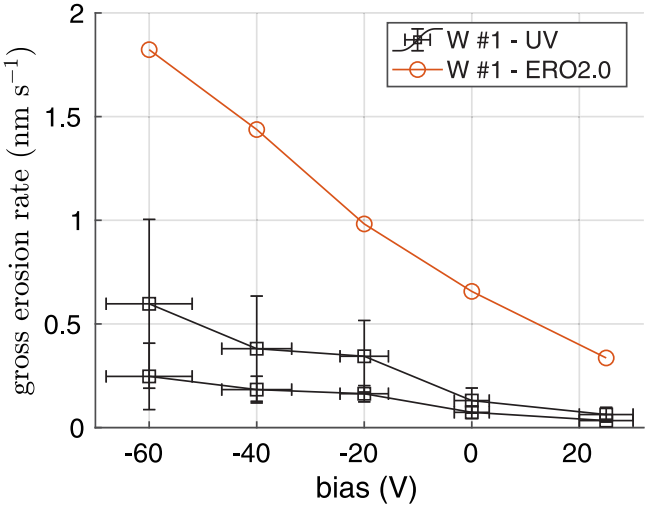

Fig. 5. UV gross erosion compared to ERO2.0 results.

ColRadPy [16], could be underestimated. The ratios between the gross erosion rate of ERO2.0 and UV signal averaged over each couple of shots appear to be relatively constant (~5) with a slightly increasing trend for larger biases (more positive), across the inspected range.

5. Conclusions

An experiment was performed in the lower divertor of DIII-D to measure the effect of DC bias on the erosion of W targets of different sizes. The goal was to compare the experimental observations with numerical results reproduced with the ERO2.0 code. Erosion post-mortem RBS measurements of W coatings No. 2, 3, 5 and 6 were in agreement with ERO2.0 estimates both in trends and order of magnitude except made for the positive case. Contrarily, coatings No. 1 and 4 do not have a clear trend with respect to bias. These inconsistencies may be attributed to the limited cumulated erosion during the experiment, which can lead to less accurate RBS measurements, particularly under positive bias or for larger coatings where net erosion is minimal. Moreover, it is suspected that an edge effect may be contaminating the measurements of coatings No. 2 to 6 since the targets were manufactured close to the boundary between the biased and unbiased sample regions. The edge effect was not included in ERO2.0 because only the biased surface was simulated. Gross erosion UV measurements are qualitatively in agreement with numerical results showing a nearly constant scaling factor of 5 when compared to the numerical findings. Finally, it can be concluded from the experiment that it is possible to qualitatively and quantitatively reproduce erosion as a function of bias at least for negative biases with ERO2.0. In the future, further studies should be performed to numerically reproduce the erosion of positively biased targets adopting longer exposure times.

CRediT authorship contribution statement

L. Cappelli: Conceptualization, Methodology, Software, Validation, Investigation, Writing – review & editing, Visualization. **J. Guterl:** Conceptualization, Methodology, Investigation, Resources, Writing – original draft, Supervision, Project administration, Funding acquisition. **N. Fedorczak:** Conceptualization, Investigation, Supervision. **D.L. Rudakov:** Investigation, Resources, Writing – original draft, Visualization. **G. Sinclair:** Investigation, Supervision, Writing – original draft, Visualization. **T. Abrams:** Conceptualization, Investigation, Writing – original draft. **S. Di Genova:** Investigation, Software. **U. Losada:** Investigation. **I. Bykov:** Investigation, Resources. **Ž. Popović:** Investigation. **D. Truong:** Investigation. **J. Watkins:** Investigation. **R.S. Wilcox:** Investigation. **W.R. Wampler:** Resources. **E. Serre:** Funding acquisition.

Declaration of competing interest

The authors declare the following financial interests/personal relationships which may be considered as potential competing interests: Luca Cappelli reports financial support, equipment, drugs, or supplies, and writing assistance were provided by DIII-D National Fusion Facility.

Data availability

Data will be made available on request.

Acknowledgments

This work has been supported by the French National Research Agency grant SISTEM (ANR-19-CE46-0005-03) and has received funding from the Excellence Initiative of Aix-Marseille University - A*Midex, a French "Investissements d'Avenir" program AMX-19-IET-013. This work has been carried out within the framework of the EUROfusion Consortium, funded by the European Union via the Euratom Research and Training Programme (Grant Agreement No 101052200 - EUROfusion). Views and opinions expressed are however those of the authors only and do not necessarily reflect those of the European Union or the European Commission. Neither the European Union nor the European Commission can be held responsible for them. This material is based upon work supported by the U.S. Department of Energy, Office of Science, Office of Fusion Energy Sciences, using the DIII-D National Fusion Facility, a DOE Office of Science user facility, under Awards DE-SC0018423 and DE-FC02-04ER54698".

Disclaimer

References

[1] V. Philipps, J. Roth, A. Loarte, Key issues in plasma–wall interactions for ITER: a European approach, Plasma Phys. Control. Fusion 45 (12A) (2003) A17.

[2] J. Romazanov, S. Brezinsek, D. Borodin, M. Groth, S. Wiesen, A. Kirschner, A. Huber, A. Widdowson, M. Airila, A. Eksaeva, et al., Beryllium global erosion and deposition at JET-ILW simulated with ERO2. 0, Nucl. Mater. Energy 18 (2019) 331–338.

[3] A. Chankin, D. Coster, R. Dux, Monte Carlo simulations of tungsten redeposition at the divertor target, Plasma Phys. Control. Fusion 56 (2) (2014) 025003.

[4] C. Wong, D. Whyte, R. Bastasz, J. Brooks, W. West, W. Wampler, Divertor materials evaluation system (DiMES), J. Nucl. Mater. 258 (1998) 433–439.

[5] R. Ding, D. Rudakov, P. Stangeby, W. Wampler, T. Abrams, S. Brezinsek, A. Briesemeister, I. Bykov, V. Chan, C. Chrobak, et al., Advances in understanding of high-Z material erosion and re-deposition in low-Z wall environment in DIII-D, Nucl. Fusion 57 (5) (2017) 056016.

[6] P. Stangeby, D. Rudakov, W. Wampler, J. Brooks, N. Brooks, D. Buchenauer, J. Elder, A. Hassanein, A. Leonard, A. McLean, et al., An experimental comparison of gross and net erosion of Mo in the DIII-D divertor, J. Nucl. Mater. 438 (2013) S309–S312.

[7] S. Abe, C. Skinner, I. Bykov, Y. Yeh, A. Lasa, J. Coburn, D. Rudakov, C. Lasnier, H. Wang, A. McLean, et al., Experimental verification of ion impact angle distribution at divertor surfaces using micro-engineered targets on DiMES at DIII-D, Nucl. Mater. Energy 27 (2021) 100965.

[8] M.W. Thompson, II. The energy spectrum of ejected atoms during the high energy sputtering of gold, Phil. Mag. 18 (152) (1968) 377–414.
[9] P.C. Stangeby, The Plasma Boundary of Magnetic Fusion Devices, Institute of Physics Pub., Philadelphia, Pennsylvania, 2000.
[10] I. Borodkina, D. Borodin, A. Kirschner, I. Tsvetkov, V. Kurnaev, M. Komm, R. Dejarnac, J. Contributors, An analytical expression for the electric field and particle tracing in modelling of Be erosion experiments at the JET ITER-like wall, Contrib. Plasma Phys. 56 (6–8) (2016) 640–645.
[11] P. Stangeby, The Chodura sheath for angles of a few degrees between the magnetic field and the surface of divertor targets and limiters, Nucl. Fusion 52 (8) (2012) 083012.
[12] T. Abrams, R. Ding, H.Y. Guo, D.M. Thomas, C.P. Chrobak, D.L. Rudakov, A.G. McLean, E.A. Unterberg, A.R. Briesemeister, P.C. Stangeby, et al., The inter-ELM tungsten erosion profile in DIII-D H-mode discharges and benchmarking with ERO+ OEDGE modeling, Nucl. Fusion 57 (5) (2017) 056034.
[13] A. Eksaeva, E. Marenkov, D. Borodin, A. Kreter, M. Reinhart, A. Kirschner, J. Romazanov, A. Terra, S. Brezinsek, K. Nordlund, ERO modelling of tungsten erosion in the linear plasma device PSI-2, Nucl. Mater. Energy 12 (2017) 253–260.
[14] J. Guterl, I. Bykov, R. Ding, P. Snyder, On the prediction and monitoring of tungsten prompt redeposition in tokamak divertors, Nucl. Mater. Energy 27 (2021) 100948.
[15] D. Rudakov, P. Stangeby, W. Wampler, J. Brooks, N. Brooks, J. Elder, A. Hassanein, A. Leonard, A. McLean, R. Moyer, et al., Net versus gross erosion of high-Z materials in the divertor of DIII-D, Phys. Scr. 2014 (T159) (2014) 014030.
[16] C. Johnson, S. Loch, D. Ennis, The effect of metastable atomic levels in neutral tungsten for erosion and impurity transport applications, Plasma Phys. Control. Fusion 62 (12) (2020) 125017.